Angewandte Chemie
Eine Zeitschrift der Gesellschaft Deutscher Chemiker

Supporting Information

Optical Spin Polarization of a Narrow-Linewidth Electron-Spin Qubit in a Chromophore/Stable-Radical System

Y. Qiu, A. Equbal, C. Lin, Y. Huang, P. J. Brown, R. M. Young, M. D. Krzyaniak, M. R. Wasielewski**

Table of Contents

Synthetic Procedures and Characterization.

General. Chemicals were purchased from Sigma-Aldrich, Inc. unless noted otherwise. ^{1}H and ^{13}C NMR spectra were acquired using a 500 MHz Bruker Avance III NMR spectrometer equipped with DCH CryoProbe. Mass spectra were collected using a Bruker RapiFlex MALDI-TOF. Purification was performed using silica gel from Sorbent Technologies (Atlanta, GA).

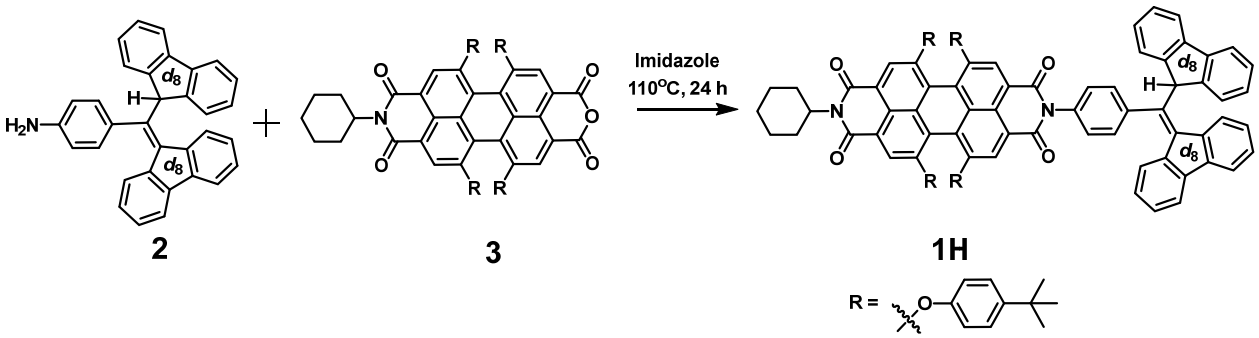

Scheme S1. Synthesis route of compound **1H**.

Compound 1H. Detailed synthesis descriptions of both **2** and **3** were reported previously.[1-2] In a flame-dried two-neck round bottle flask, **2** (23 mg, 50 μmol), **3** (52 mg, 49 μmol), and solid imidazole (2g) were added with a magnetic stirring bar. The mixture was immediately purged with three cycles of vacuum and nitrogen gas to prevent the subsequent oxidation to BDPA-d_{16} radical from the possible deprotonation of BDPAH-d_{16}, then it was heated to 110 ºC with vigorous stirring for additional 16 hours while imidazole melted completely. The mixture was cooled down to room temperature and a degassed 10% (v/v) AcOH solution in DCM (20 mL) was added through a rubber septum for neutralization (to avoid the deprotonated BDPAH-d_{16} being exposed to the air) followed by 20 mL of H_2O. The organic layer was separated, washed with H_2O (3 x 20 mL), dried over sodium sulfate, and then evaporated to dryness before the crude mixture was purified using column chromatography on silica gel with 1:1 Hexane: DCM eluent (R_f=0.47) to collect a red solid as the final product **1H** (54 mg, 36 μmol, 73%).^{1}H-NMR (500 MHz, $CDCl_3$): δ = 8.19 (s, 2H), 8.18 (s, 2H), 7.19–7.24 (m, 8H), 6.88 (d, J = 8.1 Hz, 2H), 6.77–6.83 (m, 10H), 6.48 (s, 1H), 4.88–

5.00 (m, 1H), 2.37–2.50 (m, 2H), 1.80–1.86 (m, 2H), 1.64–1.70 (m, 3H), 1.35–1.41 (m, 3H), 1.28 (s, 18H), 1.27 (s, 18H). ^{13}C-NMR (126 MHz, $CDCl_3$): δ = 163.84, 163.34, 156.10, 155.80, 152.82, 152.77, 147.22, 147.19, 143.94, 143.75, 141.89, 141.30, 139.59, 139.07, 138.55, 138.48, 136.51, 134.15, 133.07, 132.77, 129.31, 128.08, 126.68, 126.64, 123.06, 122.25, 128.87, 120.13, 120.05, 119.73, 119.70, 119.36, 119.32, 119.27, 53.92, 52.42, 34.35, 31.44, 31.43, 29.07, 26.47, 25.41. MS (MALDI-TOF) m/z: [M^+] calculated $C_{103}H_{72}D_{16}N_2O_8$, 1497.76; found 1497.38.

***Generation of radical* 1.** Generation of the desired radical tpPDI-BDPA-d_{16} (**1**) from **1H** was performed (right before experimental measurements) using MnO_2 and 1,5-diazabicyclo(4.3.0)non-5-ene (DBU) in dry THF by procedures described before.[1] The resulting THF solution of **1** were evaporated to dryness using a stream of N_2 before being dissolved in toluene or mTHF for further measurements. The successful generation and purity of the BDPA-d_{16} radical were confirmed through the ^{1}H NMR spectrum, by the disappearance of protons corresponding to BDPAH-d_{16} and broadened peaks of protons on the phenyl ring adjacent to the radical center (Figure S1). The existence of the radical was also confirmed by MS (MALDI-TOF) m/z: [M^+] calculated $C_{103}H_{71}D_{16}N_2O_8$, 1496.75; found 1496.75.

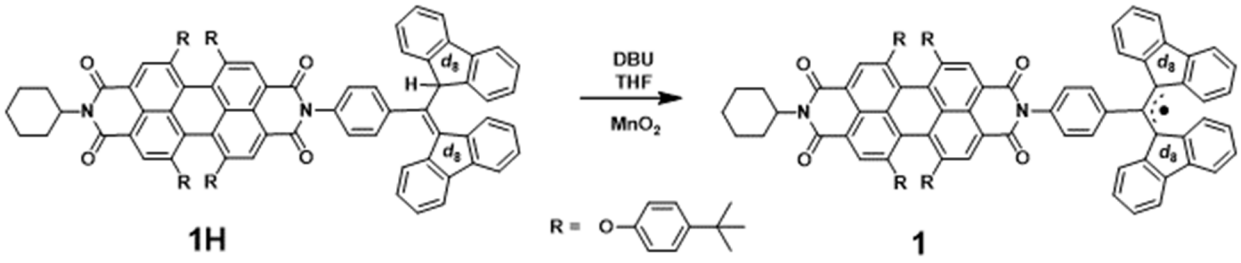

Scheme S2. Preparation of **1**.

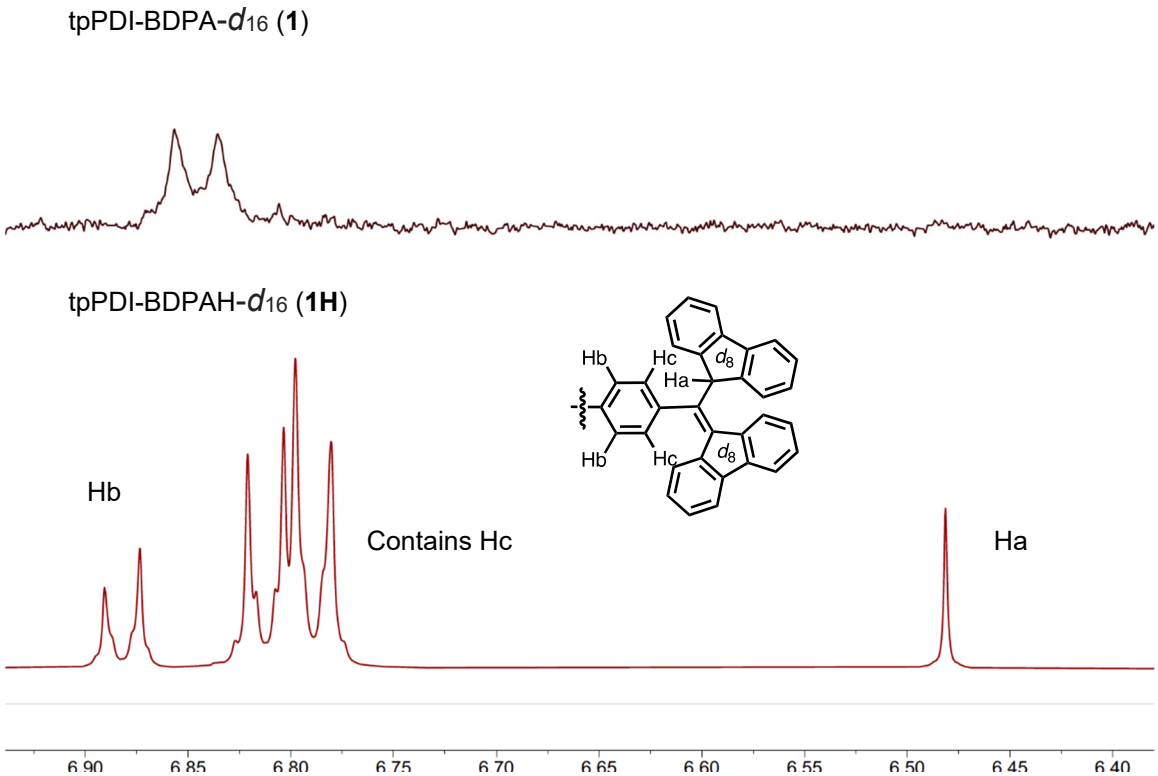

Figure S1. ^{1}H NMR verification of the successful preparation of radical **1**. The bottom and top spectra are for **1H** and **1**, respectively. By comparison, the disappearance of the Ha signal of **1H** suggests the deprotonation and the subsequent oxidation to the BDPA-d_{16} radical. Broadened peaks of Hb and Hc are also indicative of the radical generation.

Experimental Measurement Details

Sample Preparation.

Room temperature femtosecond and nanosecond transient absorption (fsTA and nsTA) optical experiments were performed in toluene solutions, which were prepared in 2 mm path length glass cuvettes and degassed with three freeze−pump−thaw cycles. Low temperature experiments were performed in glassy 2-methyltetrahydrofuran (mTHF) solution at 85 K. The mTHF was distilled, deoxygenated, and stored in the glove box in which the sample solutions were prepared. The low temperature sample cell, composed of two quartz windows separated by a Teflon spacer (~2 mm), was filled with the solution, and assembled under inert gas atmosphere in the glove box. The sample concentration was adjusted to have an optical density (O.D.) of about 0.3−0.6 at the excitation wavelength in the sample cuvette. For all EPR measurements, the samples were prepared with an absorbance of roughly 1 O.D. at the excitation wavelength of 545 nm, measured in a 2 mm cuvette. Solutions (~30 μL) were loaded into quartz tubes (2.40 mm outer diameter, 2.00 mm inner diameter), subjected to three freeze-pump-thaw cycles on a vacuum line (10^{-4} Torr), and sealed with a hydrogen torch. For low temperature experiments, the samples were pre-frozen in liquid nitrogen before inserting them into the pre-cooled resonator at 85 K.

Steady-State Absorption and Emission Spectroscopy.

Steady-state absorption spectra were acquired on a Shimadzu 1800 spectrophotometer. Steady-state fluorescence spectra were collected on a Horiba Nanolog fluorometer set to right-angle detection mode. All measurements were performed in toluene at room temperature.

Transient Absorption Spectroscopy.

The femtosecond transient absorption (fsTA) and nanosecond transient absorption (nsTA) experiments were conducted using a previously described instrument.[3-4] Both measurements were

performed by using a regeneratively amplified Ti:sapphire laser system operating at 1 kHz repetition rate to generate 828 nm pulses, which generate the 545 nm excitation pulses using a commercial collinear optical parametric amplifier (TOPAS-Prime, Light Conversion, LLC). Low temperature fsTA and nsTA experiments were performed in a Janis VNF-100 cryostat (Lakeshore Cryotronics) using a Cryo-Con 32B (Cryogenics Control Systems, Inc.) temperature controller. All TA spectra were acquired by using an excitation energy of about 1 μJ/pulse. The data were background-subtracted and chirp-corrected using a lab-written MATLAB program. The TA data was subjected to global kinetic analysis to obtain the evolution-associated and kinetic parameters as described in detail previously.[5]

Electron Paramagnetic Resonance (EPR) spectroscopy.

All EPR measurements at X-band were made on a Bruker Elexsys E680 X/W EPR spectrometer equipped with a 3 mm split ring resonator (ER4118X-MS3) (~9.5 GHz) or a 5 mm dielectric resonator (ER4118X-MD5) (~9.8 GHz). The temperature was controlled by an Oxford Instruments CF935 continuous flow optical cryostat using liquid nitrogen.

Transient Continuous-Wave (CW) EPR Spectroscopy. For transient CW EPR studies, the sample was photoexcited at 545 nm with 7 ns pulses generated via an optical parametric oscillator (Spectra-Physics BasiScan) pumped with the 355 nm output of a frequency-tripled Nd:YAG laser (Spectra-Physics Quanta-Ray Lab-150 or Lab-170-10H) operating at a repetition rate of 10 Hz. The laser light was coupled into the resonator with a fiber optic and collimator placed outside the cryostat window resulting in about 0.8 mJ passing into the resonator and exciting the sample. Following photoexcitation, time traces of the transient magnetization were acquired as a function of the magnetic field using quadrature detection under continuous microwave irradiation of 1.5 mW. The data were processed by first subtracting the background signal prior to the laser pulse

for each kinetic trace (at a given magnetic field) and then subtracting the signal at off-resonance magnetic fields for each spectrum (at any given time). The data were processed in MATLAB utilizing a number of functions from the EasySpin software package.[6]

Pulse-EPR Spectroscopy. Echo-detected field-swept (EDFS) EPR spectra were recorded by using the pulse sequence: $h\nu$-T_{DAF}-$\pi/2$-τ-π-τ-echo, with τ = 250 ns, $\pi/2$ and π-pulse lengths of 12 and 24 ns, respectively. The same pulse sequence was used with a delay after laser flash T_{DAF} = 10 μs for the determination of the phase memory time, T_m, which is closely related to the coherence time, T_2, by varying the value of τ. T_m was extracted by fitting the echo intensity decay, I, with a monoexponential function $I = I_0 \times e^{-2\tau/T_m}$, where I_0 is the echo intensity at τ = 0. The polarization lifetimes were measured using the same basic pulse scheme but varying the position of the laser pulse (T_{DAF}) with respect to the echo detection pulses. Transient nutation measurements used the pulse sequence: $h\nu$-T_{DAF}-p_{nut}-τ_{wait}-$\pi/2$-τ-π-τ-echo where T_{DAF} = 10 μs, τ = 200 ns, and $\pi/2$ and π-pulse lengths of 12 and 24 ns, respectively. The length (T_{nut}) of the nutation pulse (p_{nut}) was gradually increased in steps of 4 ns, starting at 0 ns with τ_{wait} = 2 μs. Pulse artefacts were removed using 8-step phase cycling. The nutation frequency amplitudes were calculated from the discrete Fourier transformation (FT) of the time-domain oscillations. The amplitudes of FT spectra (y-axis) were self-normalized, and the frequency (x-axis) were normalized by the nutation frequency axis measured for the dark state of the same sample (i.e. S = 1/2 for the BDPA-d_{16} radical).

Computation Details.

All calculations were performed using QChem 5.1.[7] Input geometries were constructed in Avogadro software and pre-optimized by using the MMFF94 force field.[8] *Tert*-butyl groups and deuteration were omitted to save computational expense, and the cyclohexyl group was replaced with an isopropyl group for the same purpose. Geometry optimizations and spin density

calculations were performed by using Density Functional Theory (DFT) at B3LYP/3-21G(d) level of theory. All optimized geometries were found to have zero imaginary frequencies. Visualization of the spin densities uses IQmol software.

Spin Densities.

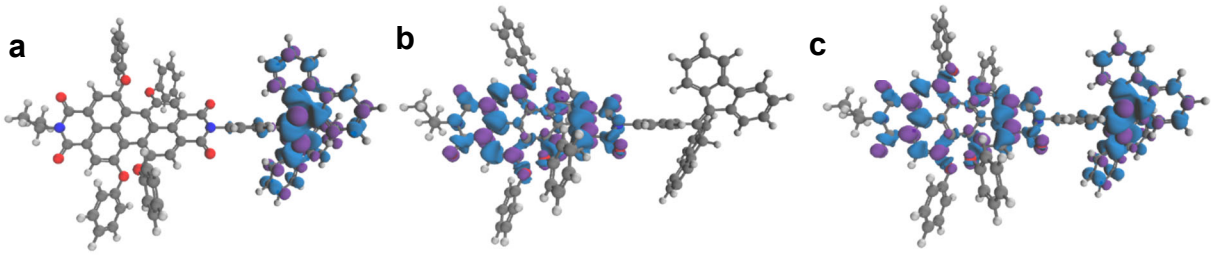

Figure S2. Spin densities in (a) ground state doublet of **1,** (b) the excited triplet state of **1H**, and (c) the quartet state of **1**.

Transient Absorption Spectra at 85 K in mTHF.

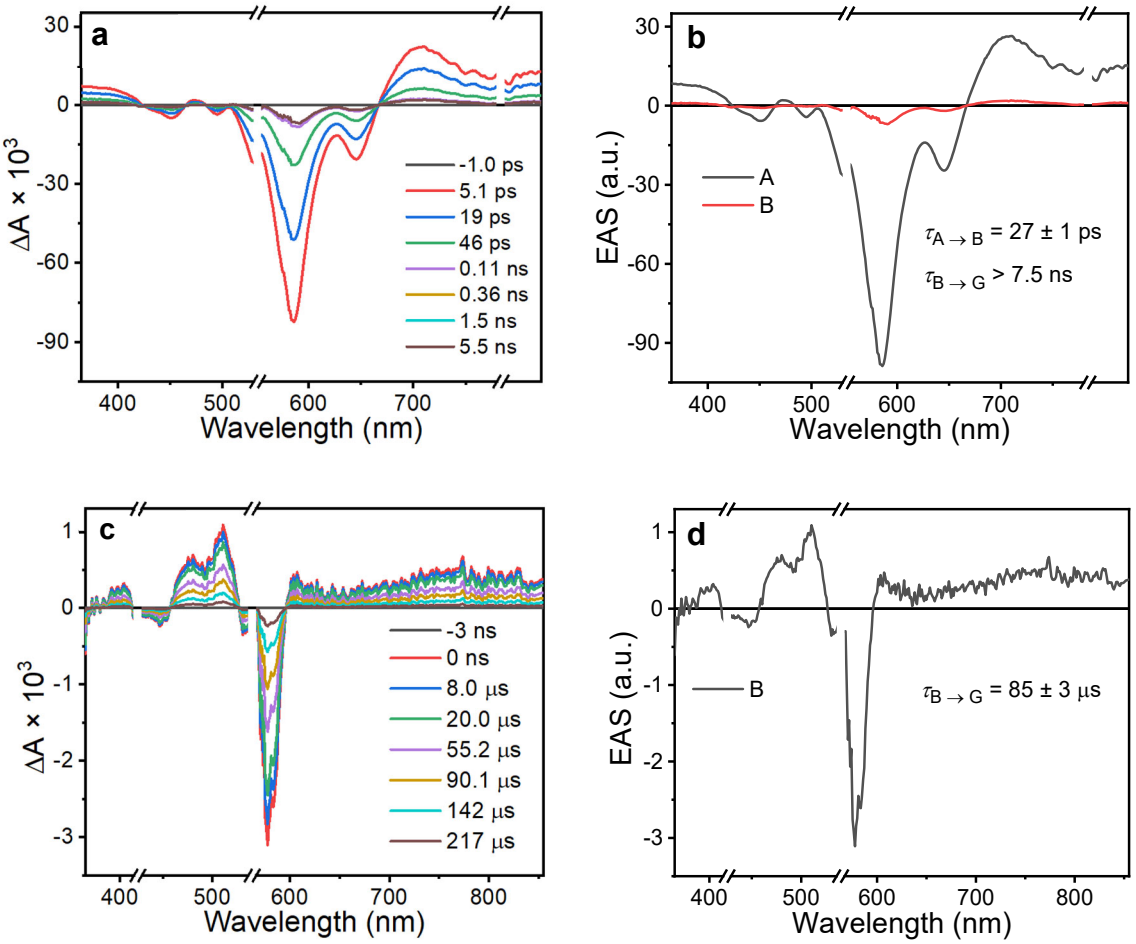

Figure S3. (a) FsTA spectra of **1** in mTHF at 85 K following 545 nm excitation. (b) Evolution-associated spectra and kinetic values. (c) NsTA spectra of **1** in mTHF at 85 K following 545 nm excitation. (d) Evolution-associated spectra and kinetic values.

Reverse Quartet Mechanism (RQM).

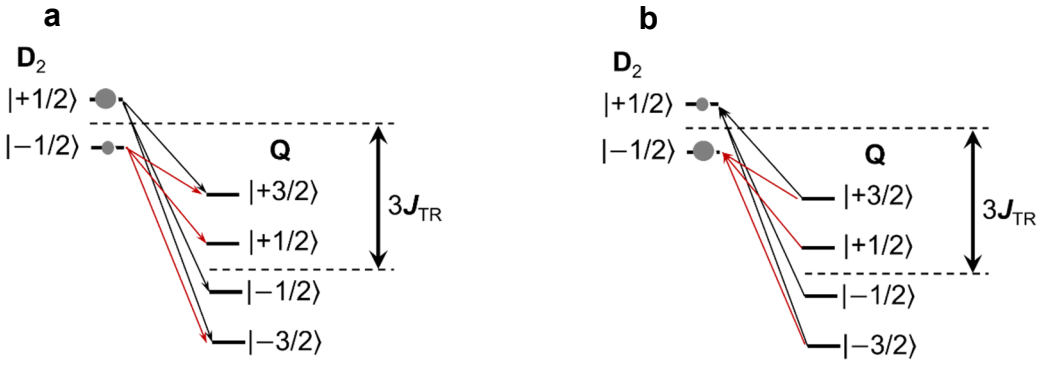

Figure S4. In the scheme of reverse quartet mechanism, when $J_{TR} > 0$, the polarization pattern is (a) emissive at early time and (b) absorptive at later times.

For $J_{TR} > 0$, among all spin-allowed transitions between spin sublevels ($\Delta m_S = \pm 1, \pm 2$). $|\mathbf{D}_2(-1/2)\rangle \rightarrow |\mathbf{Q}(+3/2)\rangle$ is most favored because of the smallest energy gap, resulting in faster depletion of $|\mathbf{D}_2(-1/2)\rangle$ at early times and an overpopulation of $|\mathbf{D}_2(+1/2)\rangle$. The decay from $\mathbf{D}_2$ to $\mathbf{D}_0$ carries the same population distribution and should yield an emissive signal. At later times, **Q** relaxes to $\mathbf{D}_0$ via the $|\mathbf{D}_2(-1/2)\rangle$ sublevel due to the smaller energy gaps, which should produce an absorptive polarization feature of $\mathbf{D}_0$. For $J_{TR} < 0$, a similar mechanistic picture is expected, except that the spin manifold of **Q** is now energetically above that of $\mathbf{D}_2$, and the two states closest in energy are $|\mathbf{D}_2\ (+1/2)\rangle$ and $|\mathbf{Q}(-3/2)\rangle$. The polarization exhibits an absorptive feature at early times and emissive at later times.

DFT-Calculation Coordinates.

tpPDI-BDPA

Spin Multiplicity: 4

Charge: 0

Cartesian Coordinates:

O	9.539519	-2.3159	0.394018
C	8.909393	-1.25816	0.179613
N	9.562985	-0.0437	-0.07629
C	8.90896	1.187302	-0.30198
C	7.438534	-1.22942	0.180866
C	6.738893	-0.02619	-0.02592
C	7.440909	1.171609	-0.25381
C	6.746671	-2.41103	0.468977
C	5.366852	-2.42812	0.463723
C	4.60797	-1.26089	0.087114
C	5.311372	-0.02091	-0.00559
C	4.614401	1.223952	-0.08062
C	5.371005	2.385876	-0.47751
C	6.749821	2.358891	-0.52118
C	3.203665	-1.25134	-0.14438
C	2.508116	-0.01104	0.025798
C	3.215944	1.22397	0.182432
O	9.54806	2.233006	-0.53335
C	1.078322	-0.00468	0.036738
C	0.385846	1.177601	0.350724
C	1.087266	2.334207	0.711445
C	2.46397	2.364117	0.666168
C	2.433687	-2.38543	-0.61371
C	1.056698	-2.34332	-0.63758
C	0.370833	-1.18028	-0.26814
C	-1.09556	-1.20555	-0.28942
N	-1.75166	0.009947	0.05002
C	-1.07986	1.217551	0.38707
O	-1.70697	2.243162	0.703566
O	-1.73606	-2.22529	-0.5978
O	4.627561	3.455877	-0.94387
O	3.194234	3.434862	1.1685
C	11.06922	-0.01807	-0.1236
C	11.66675	-0.38468	1.247916

C	11.59688	-0.91987	-1.25587
C	-3.20031	0.019103	0.050021
C	-3.90555	-0.464	-1.05772
C	-5.29758	-0.44906	-1.05934
C	-6.00823	0.037536	0.047398
C	-5.29333	0.515078	1.155206
C	-3.90106	0.511673	1.156322
C	-7.50584	0.044851	0.04645
C	-8.15989	0.698131	-1.0192
C	-8.16669	-0.60379	1.110812
C	-9.45178	-0.21824	1.724412
C	-9.71181	-1.07376	2.835779
C	-8.60736	-2.04261	2.932301
C	-7.65763	-1.73267	1.911659
C	-10.307	0.853886	1.457712
C	-11.4313	1.044608	2.266118
C	-11.6969	0.186527	3.340113
C	-10.8313	-0.87509	3.636201
C	-8.40761	-3.12227	3.784378
C	-7.25927	-3.90984	3.623662
C	-6.33423	-3.62281	2.61304
C	-6.5265	-2.54058	1.749318
C	-9.44703	0.322649	-1.63469
C	-9.69727	1.17814	-2.74839
C	-8.58418	2.137166	-2.84447
C	-7.63946	1.821015	-1.82115
C	-10.312	-0.74154	-1.36775
C	-11.4362	-0.9242	-2.17821
C	-11.6921	-0.066	-3.25445
C	-10.8167	0.987492	-3.55083
C	-8.37309	3.213422	-3.69812
C	-7.2184	3.991435	-3.53615
C	-6.29817	3.698361	-2.52286
C	-6.50179	2.619365	-1.65769
O	4.628812	-3.49315	0.949544
O	3.145166	-3.46383	-1.1272
C	5.113059	4.779715	-0.88045
C	2.5432	4.372257	2.021014
C	4.985017	5.553778	-2.03203
C	5.402613	6.884907	-2.00908
C	5.953447	7.42959	-0.84591
C	6.072614	6.641165	0.302048
C	5.647379	5.312311	0.2928
C	2.296647	5.654804	1.542134
C	1.704677	6.592408	2.391778

C	1.360013	6.240802	3.699132
C	1.612474	4.946743	4.16268
C	2.20455	4.003913	3.321979
H	7.320901	-3.28963	0.728065
H	7.32204	3.233403	-0.79785
H	0.521745	3.188249	1.056064
H	0.47874	-3.19236	-0.97391
H	11.29088	1.02486	-0.35274
H	11.40445	-1.41232	1.502974
H	11.29001	0.291809	2.022124
H	12.7571	-0.28781	1.201953
H	11.3332	-1.95894	-1.05441
H	12.68684	-0.82464	-1.3113
H	11.17181	-0.61358	-2.21741
H	-3.36717	-0.86978	-1.90047
H	-5.84302	-0.81614	-1.91994
H	-5.83543	0.889006	2.014943
H	-3.35896	0.910544	1.999925
H	-10.1065	1.522154	0.631902
H	-12.1031	1.86927	2.059088
H	-12.5738	0.35167	3.955392
H	-11.0272	-1.52056	4.485182
H	-9.13149	-3.36079	4.555513
H	-7.09097	-4.75395	4.282437
H	-5.45643	-4.2472	2.495175
H	-5.8063	-2.3335	0.970573
H	-10.1192	-1.40998	-0.54029
H	-12.1156	-1.74258	-1.97093
H	-12.5691	-0.22479	-3.87128
H	-11.0051	1.632903	-4.40152
H	-9.09306	3.456779	-4.47145
H	-7.04133	4.832811	-4.19613
H	-5.41532	4.315421	-2.4041
H	-5.78518	2.407191	-0.87695
H	4.56174	5.103735	-2.91995
H	5.306964	7.491249	-2.90178
H	6.28582	8.460384	-0.83363
H	6.48926	7.061047	1.209658
H	5.707562	4.697761	1.18046
H	2.58164	5.907167	0.53013
H	1.510038	7.594332	2.028732
H	0.897432	6.970124	4.35285
H	1.348231	4.66932	5.175974
H	2.407323	2.997652	3.665159
C	5.095776	-4.82206	0.861152

C	5.597889	-5.3491	-0.32868
H	5.648117	-4.7261	-1.211
C	6.003183	-6.68382	-0.36152
H	6.394095	-7.09919	-1.28256
C	5.896107	-7.48358	0.779739
H	6.212691	-8.51894	0.749081
C	5.377963	-6.94396	1.960172
H	5.291903	-7.55877	2.848048
C	4.980683	-5.60721	2.006607
H	4.582458	-5.16134	2.908115
C	2.473793	-4.38852	-1.97781
C	2.224383	-5.67314	-1.50613
C	1.612261	-6.59883	-2.3547
C	1.250716	-6.23344	-3.6536
C	2.118649	-4.00656	-3.27047
C	1.506475	-4.93743	-4.10998
H	2.324128	-2.99906	-3.60834
H	0.772352	-6.95338	-4.30637
H	1.22922	-4.6493	-5.1168
H	1.415105	-7.6022	-1.99705
H	2.522121	-5.93643	-0.5006

tpPDI-BDPA$^{\bullet}$

Spin Multiplicity: 2

Charge: 0

Cartesian Coordinates:

O	9.577612	-2.11512	0.659816
C	8.941512	-1.09296	0.34331
N	9.585255	0.107064	0.005236
C	8.921375	1.304696	-0.34189
C	7.46153	-1.08726	0.306542
C	6.750138	0.086148	-0.01359
C	7.443179	1.272952	-0.32455
C	6.78079	-2.23601	0.645645
C	5.37786	-2.27957	0.577165
C	4.639029	-1.17397	0.121902
C	5.3295	0.073187	-0.02009
C	4.618162	1.307625	-0.16633

C	5.340567	2.427548	-0.61332
C	6.744738	2.410105	-0.66823
C	3.206791	-1.18866	-0.16006
C	2.492266	0.047688	-0.02958
C	3.183913	1.296783	0.105712
O	9.551264	2.33188	-0.64465
C	1.069924	0.034592	-0.03243
C	0.358734	1.212007	0.267493
C	1.038907	2.364477	0.595424
C	2.44118	2.411042	0.540507
C	2.486812	-2.317	-0.59718
C	1.084285	-2.29629	-0.65786
C	0.381824	-1.15618	-0.33357
C	-1.0935	-1.20361	-0.35668
N	-1.76716	0.007268	-0.03376
C	-1.11738	1.231332	0.288314
O	-1.76172	2.246784	0.582359
O	-1.71796	-2.23107	-0.65201
O	4.628548	3.513541	-1.10266
O	3.124226	3.558197	0.933731
C	11.09338	0.155223	0.007648
C	11.64316	-0.08314	1.426535
C	11.67516	-0.8272	-1.0263
C	-3.21675	-0.00792	-0.03079
C	-3.91634	-0.49974	-1.13769
C	-5.30851	-0.51028	-1.13402
C	-6.02364	-0.03791	-0.02403
C	-5.3134	0.449109	1.082895
C	-3.92133	0.468519	1.079685
C	-7.52124	-0.0497	-0.02211
C	-8.18418	0.590363	-1.09053
C	-8.17343	-0.69767	1.047913
C	-9.46093	-0.32011	1.661538
C	-9.70793	-1.16692	2.782551
C	-8.59274	-2.12285	2.885125
C	-7.65016	-1.81351	1.85778
C	-10.3285	0.739949	1.38691
C	-11.452	0.926981	2.19736
C	-11.7046	0.077232	3.281052
C	-10.8266	-0.97193	3.584961
C	-8.37835	-3.19145	3.74747
C	-7.22249	-3.96872	3.590223
C	-6.30469	-3.68291	2.572662
C	-6.51176	-2.61171	1.6987
C	-9.46734	0.195545	-1.70245

C	-9.72914	1.041782	-2.82046
C	-8.62832	2.01408	-2.92294
C	-7.67884	1.715761	-1.89861
C	-10.3189	-0.87784	-1.42903
C	-11.4412	-1.07896	-2.23767
C	-11.7084	-0.22994	-3.31844
C	-10.8465	0.832819	-3.62109
C	-8.43154	3.087614	-3.78334
C	-7.28641	3.880783	-3.6274
C	-6.36197	3.605687	-2.61291
C	-6.55144	2.529803	-1.7407
O	4.682644	-3.3782	1.06257
O	3.193463	-3.45131	-0.9848
C	5.070367	4.838078	-0.90717
C	2.471611	4.497407	1.779451
C	4.856693	5.728017	-1.9591
C	5.22971	7.064508	-1.81062
C	5.821741	7.502982	-0.62291
C	6.025866	6.599796	0.423917
C	5.64383	5.265102	0.289798
C	2.24419	5.779905	1.289546
C	1.652493	6.729471	2.125089
C	1.287533	6.391004	3.43074
C	1.521405	5.098119	3.906483
C	2.115744	4.143566	3.080516
H	7.346001	-3.10329	0.958692
H	7.295705	3.289459	-0.97298
H	0.473682	3.238826	0.886646
H	0.536164	-3.18141	-0.94928
H	11.30805	1.178896	-0.30062
H	11.38862	-1.09037	1.758824
H	11.22502	0.648856	2.125276
H	12.73265	0.031065	1.414017
H	11.42116	-1.85105	-0.74989
H	12.76467	-0.71669	-1.05218
H	11.28064	-0.60857	-2.02416
H	-3.37383	-0.89142	-1.98469
H	-5.85046	-0.88441	-1.99368
H	-5.85911	0.812355	1.944876
H	-3.38318	0.871823	1.924062
H	-10.1382	1.40203	0.553782
H	-12.1334	1.742108	1.984128
H	-12.581	0.239311	3.897772
H	-11.0124	-1.61047	4.441391
H	-9.0966	-3.4295	4.523994

H	-7.04271	-4.80397	4.257184
H	-5.42124	-4.29976	2.457406
H	-5.79728	-2.40567	0.914348
H	-10.1169	-1.53925	-0.59804
H	-12.1101	-1.90467	-2.0255
H	-12.5837	-0.40315	-3.93385
H	-11.0436	1.47094	-4.47536
H	-9.1552	3.317045	-4.55738
H	-7.12022	4.719997	-4.29289
H	-5.48701	4.23467	-2.49861
H	-5.83199	2.332571	-0.95872
H	4.405245	5.358901	-2.87032
H	5.067279	7.758687	-2.62651
H	6.118693	8.538793	-0.51327
H	6.471183	6.935465	1.352812
H	5.764205	4.565244	1.105027
H	2.547368	6.020415	0.27994
H	1.473816	7.731097	1.753049
H	0.824257	7.129739	4.073355
H	1.242284	4.830872	4.918566
H	2.305564	3.139041	3.43632
C	5.1516	-4.69401	0.871562
C	5.743208	-5.11035	-0.32027
H	5.857474	-4.40834	-1.13452
C	6.151836	-6.43754	-0.45054
H	6.611469	-6.7649	-1.37543
C	5.956057	-7.34417	0.594886
H	6.27372	-8.37414	0.488306
C	5.345816	-6.9167	1.777397
H	5.18991	-7.6136	2.592238
C	4.946164	-5.58751	1.922151
H	4.480319	-5.22666	2.829442
C	2.560705	-4.41141	-1.82224
C	2.361467	-5.69416	-1.32075
C	1.791701	-6.6641	-2.14794
C	1.420607	-6.34539	-3.45683
C	2.198237	-4.07696	-3.12666
C	1.625848	-5.05196	-3.94426
H	2.366583	-3.07173	-3.49112
H	0.974628	-7.10007	-4.09315
H	1.341657	-4.8005	-4.95896
H	1.635217	-7.66619	-1.76732
H	2.66993	-5.91854	-0.30913

tpPDI-BDPAH

Spin Multiplicity: 3

Charge: 0

Cartesian Coordinates:

O	9.457417	-2.57984	0.657225
C	8.838679	-1.50359	0.412097
N	9.54973	-0.25528	0.156744
C	8.92705	1.039424	-0.12455
C	7.326899	-1.39725	0.36026
C	6.661881	-0.15717	0.094754
C	7.415334	1.037764	-0.14026
C	6.573644	-2.56024	0.650653
C	5.17172	-2.54603	0.601707
C	4.444528	-1.33633	0.171771
C	5.208421	-0.11006	0.064146
C	4.531507	1.163921	-0.07147
C	5.352338	2.322429	-0.47368
C	6.752992	2.246797	-0.46401
C	3.025258	-1.28834	-0.09754
C	2.344851	-0.01475	0.016705
C	3.104556	1.211068	0.150561
O	9.639271	2.063575	-0.33797
C	0.890891	0.032915	-0.00098
C	0.217944	1.27271	0.235628
C	0.960964	2.436921	0.553683
C	2.362743	2.420504	0.558465
C	2.215884	-2.44509	-0.52935
C	0.816009	-2.36992	-0.55829
C	0.143513	-1.16027	-0.25357
C	-1.36879	-1.1817	-0.26368
N	-2.01835	0.124861	-0.01609
C	-1.28939	1.390052	0.225502
O	-1.89948	2.480363	0.402587
O	-2.04413	-2.23065	-0.45336
O	4.639987	3.474349	-0.89918
O	3.148054	3.52363	0.986013
C	11.06309	-0.25291	0.174355
C	11.6095	-0.61062	1.592986
C	11.63901	-1.1957	-0.92933
C	-3.48864	0.167748	0.006693
C	-4.24796	-0.56435	-0.94238

C	-5.65298	-0.52868	-0.90437
C	-6.33734	0.234666	0.074027
C	-5.5695	0.976995	1.008205
C	-4.16646	0.941097	0.985539
C	-7.85677	0.32643	0.086926
C	-8.46946	1.017705	-1.16645
C	-8.61982	-0.1492	1.124264
C	-10.1126	0.005436	1.364659
C	-10.4106	-0.44853	2.693869
C	-9.16959	-0.9998	3.302021
C	-8.10366	-0.8675	2.356949
C	-11.1766	0.478358	0.563846
C	-12.4843	0.534887	1.095854
C	-12.7544	0.117161	2.413897
C	-11.7144	-0.38875	3.220346
C	-8.97175	-1.63067	4.545294
C	-7.69897	-2.15756	4.845753
C	-6.65234	-2.06799	3.904499
C	-6.84505	-1.42993	2.659892
C	-8.78981	0.016933	-2.3152
C	-8.18052	0.444276	-3.53036
C	-7.41924	1.702918	-3.26834
C	-7.55538	2.040734	-1.89111
C	-9.55343	-1.16029	-2.27223
C	-9.7205	-1.90656	-3.46101
C	-9.1283	-1.48011	-4.66863
C	-8.3515	-0.30369	-4.7142
C	-6.66103	2.519521	-4.13331
C	-6.04372	3.673786	-3.60872
C	-6.18474	4.01014	-2.24542
C	-6.94648	3.196813	-1.37643
H	-9.39401	1.539876	-0.85599
O	4.371649	-3.65337	0.988883
O	2.938477	-3.5955	-0.94102
C	5.357437	4.320537	-1.82038
C	2.498666	4.389355	1.939175
C	5.948856	3.821622	-3.01095
C	6.512442	4.724414	-3.92933
C	6.482588	6.112722	-3.68068
C	5.881126	6.603485	-2.5049
C	5.315339	5.714399	-1.57193
C	2.626784	5.783809	1.725931
C	2.131458	6.681982	2.689791
C	1.515237	6.199887	3.861488
C	1.399597	4.810251	4.07489

C	1.892013	3.89817	3.12538
H	7.115755	-3.46994	0.940657
H	7.363411	3.118943	-0.73244
H	0.40955	3.346937	0.82432
H	0.213227	-3.24235	-0.84273
H	11.30458	0.805188	-0.06622
H	11.32395	-1.64024	1.856774
H	11.2018	0.080132	2.346296
H	12.70721	-0.53098	1.597776
H	11.34263	-2.23499	-0.72166
H	12.73739	-1.12907	-0.93698
H	11.25968	-0.90356	-1.92003
H	-3.73468	-1.1648	-1.70295
H	-6.22592	-1.10254	-1.64482
H	-6.08196	1.57747	1.771647
H	-3.59024	1.515811	1.720343
H	-11.0305	0.780453	-0.47828
H	-13.3028	0.903419	0.463128
H	-13.7789	0.169639	2.806339
H	-11.9197	-0.73851	4.240847
H	-9.7966	-1.72314	5.264424
H	-7.5265	-2.65579	5.809257
H	-5.6722	-2.50484	4.138147
H	-6.01897	-1.3872	1.941443
H	-10.0085	-1.50197	-1.33291
H	-10.3159	-2.82928	-3.44307
H	-9.2703	-2.07379	-5.58187
H	-7.88733	0.021121	-5.65504
H	-6.55254	2.263994	-5.19589
H	-5.44734	4.319352	-4.26765
H	-5.69671	4.913388	-1.85499
H	-7.05137	3.465114	-0.3166
H	5.964285	2.741166	-3.20366
H	6.973184	4.340638	-4.84985
H	6.924848	6.809476	-4.40472
H	5.853759	7.684082	-2.30941
H	4.844429	6.08108	-0.65093
H	3.107699	6.144474	0.807741
H	2.225549	7.763507	2.521645
H	1.128229	6.904195	4.609557
H	0.927582	4.432184	4.992058
H	1.810099	2.816157	3.290988
C	4.985314	-4.53213	1.953296
C	4.857696	-5.92347	1.719682
H	4.404888	-6.27102	0.782359

C	5.317755	-6.83516	2.688224
H	5.224247	-7.91418	2.50433
C	5.898189	-6.36988	3.884784
H	6.257914	-7.08494	4.636269
C	6.013145	-4.98342	4.11816
H	6.45731	-4.61828	5.05424
C	5.555476	-4.05792	3.164195
H	5.637361	-2.97835	3.344893
C	2.253397	-4.42517	-1.90132
C	2.29028	-5.82333	-1.67749
C	1.758064	-6.69571	-2.64531
C	1.195423	-6.18425	-3.83148
C	1.701049	-3.90518	-3.10171
C	1.170796	-4.79162	-4.05519
H	1.689605	-2.82139	-3.27494
H	0.779329	-6.86823	-4.58273
H	0.740392	-4.39151	-4.98341
H	1.781245	-7.77973	-2.46911
H	2.731005	-6.20646	-0.74829

References

[1] B. K. Rugg, B. T. Phelan, N. E. Horwitz, R. M. Young, M. D. Krzyaniak, M. A. Ratner, M. R. Wasielewski, *J. Am. Chem. Soc.* **2017**, *139*, 15660-15663.

[2] M. Berberich, M. Natali, P. Spenst, C. Chiorboli, F. Scandola, F. Wuerthner, *Chem. Eur. J.* **2012**, *18*, 13651-13664.

[3] R. M. Young, S. M. Dyar, J. C. Barnes, M. Juricek, J. F. Stoddart, D. T. Co, M. R. Wasielewski, *J. Phys. Chem. A* **2013**, *117*, 12438-12448.

[4] P. E. Hartnett, E. A. Margulies, H. S. S. R. Matte, M. C. Hersam, T. J. Marks, M. R. Wasielewski, *Chem. Mater.* **2016**, *28*, 3928-3936.

[5] A. F. Coleman, M. Chen, J. Zhou, J. Y. Shin, Y. Wu, R. M. Young, M. R. Wasielewski, *J. Phys. Chem. C* **2020**, *124*, 10408-10419.

[6] S. Stoll, A. Schweiger, *J. Magn. Reson.* **2006**, *178*, 42-55.

[7] Y. Shao, Z. Gan, E. Epifanovsky, A. T. B. Gilbert, M. Wormit, J. Kussmann, A. W. Lange, A. Behn, J. Deng, X. Feng, D. Ghosh, M. Goldey, P. R. Horn, L. D. Jacobson, I. Kaliman, R. Z. Khaliullin, T. Kuś, A. Landau, J. Liu, E. I. Proynov, Y. M. Rhee, R. M. Richard, M. A. Rohrdanz, R. P. Steele, E. J. Sundstrom, H. L. Woodcock, P. M. Zimmerman, D. Zuev, B. Albrecht, E. Alguire, B. Austin, G. J. O. Beran, Y. A. Bernard, E. Berquist, K. Brandhorst, K. B. Bravaya, S. T. Brown, D. Casanova, C.-M. Chang, Y. Chen, S. H. Chien, K. D. Closser, D. L. Crittenden, M. Diedenhofen, R. A. DiStasio, H. Do, A. D. Dutoi, R. G. Edgar, S. Fatehi, L. Fusti-Molnar, A. Ghysels, A. Golubeva-Zadorozhnaya, J. Gomes, M. W. D. Hanson-Heine, P. H. P. Harbach, A. W. Hauser, E. G. Hohenstein, Z. C. Holden, T.-C. Jagau, H. Ji, B. Kaduk, K. Khistyaev, J. Kim, J. Kim, R. A. King, P. Klunzinger, D. Kosenkov, T. Kowalczyk, C. M. Krauter, K. U. Lao, A. D. Laurent, K. V. Lawler, S. V.

Levchenko, C. Y. Lin, F. Liu, E. Livshits, R. C. Lochan, A. Luenser, P. Manohar, S. F. Manzer, S.-P. Mao, N. Mardirossian, A. V. Marenich, S. A. Maurer, N. J. Mayhall, E. Neuscamman, C. M. Oana, R. Olivares-Amaya, D. P. O'Neill, J. A. Parkhill, T. M. Perrine, R. Peverati, A. Prociuk, D. R. Rehn, E. Rosta, N. J. Russ, S. M. Sharada, S. Sharma, D. W. Small, A. Sodt, et al., *Mol. Phys.* **2015**, *113*, 184-215.

[8] M. D. Hanwell, D. E. Curtis, D. C. Lonie, T. Vandermeersch, E. Zurek, G. R. Hutchison, *J. Cheminformatics* **2012**, *4*, 17.